

# Enhancement of Non-Destructive Measurement Resolution with Neural Networks

Ergun Simsek and Emerson K. Cho

University of Maryland Baltimore County, Baltimore, MD, USA (simsek@umbc.edu)

**Abstract**—Similar to image sharpening, the resolution of measured electromagnetic fields can be enhanced with machine learning. We numerically demonstrate that a  $\lambda/10$  spatial resolution is achievable even with probes that are a few wavelengths wide, while maintaining a maximum relative error of less than 3%.

## I. INTRODUCTION

In the ever-evolving landscape of modern technology, the demand for high-performance microwave and photonic devices has surged, driven by applications ranging from communication systems to medical devices. Ensuring the optimal functioning of these devices requires a thorough understanding of their electromagnetic properties, particularly the electric fields at the micro and nanoscale. Local near-field probing (LNFP) [1]–[3] emerges as a powerful and indispensable technique for measuring electric fields in these devices, providing valuable insights into their performance and aiding in the advancement of cutting-edge technologies.

Near-field probing involves the measurement of electromagnetic fields in close proximity to a source, offering advantages over traditional far-field techniques. In the context of microwave and photonic devices, local near-field probing allows us to investigate the intricate details of electric fields with high spatial resolution. This technique is especially crucial as devices continue to shrink in size, making traditional measurement methods less effective due to diffraction limitations. Despite its numerous advantages, local near-field probing faces challenges such as potential perturbations introduced by the probing process and blurring for nano- and micro-scale devices under investigation. These errors in measurements (due to perturbations and blurring) can be quantified with the help of commercially available numerical solvers that solve Maxwell’s and circuit equations simultaneously. In this work, we are interested in removing these errors with machine learning.

The general idea behind our approach is—in fact—very similar to image sharpening. As illustrated in Fig. 1 (a), when trained with large-enough data sets, the machine learning algorithms can successfully sharpen images [4]. In this work, we utilize neural networks to achieve a similar resolution enhancement on a hypothetical scenario illustrated in Fig. 1 (b) where the measured data is perturbed and blurred.

We assume that the size of the probe used for the LNFP exceeds the dimensions of the device under investigation. Since LNFP resolution is compromised due to the limitations of the probe and the probe-device distance, true electric field intensities become blurred when measured with this large probe. To mimic this scenario we first calculated the true electric field distributions over 2330 unique modified uni-traveling

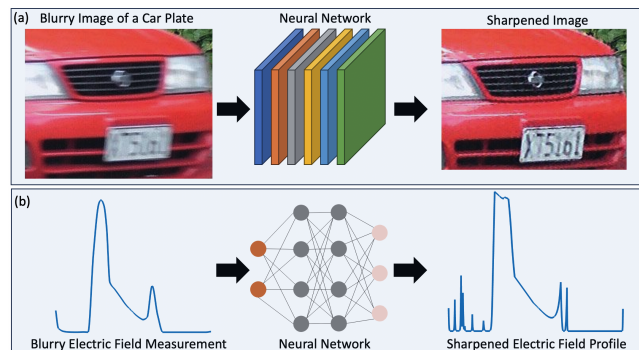


Fig. 1. An analogy between (a) image sharpening and (b) measurement resolution sharpening using neural networks.

wave carrier photodetectors using a drift-diffusion equation solver [5]. Then, we created synthetic electric field profiles, expected to be measured by a probe, using a Green’s function formalism [6]. The dataset, including true and measured blurry electric field distributions, can be found at [9].

## II. IMPLEMENTATION AND RESULTS

Our study evaluates two ML methods, linear regression and fully connected neural networks (FCNNs), to predict electric field profiles for different scenarios. In the first scenario, we standardize the thickness of each photodetector layer to achieve a uniform device length of  $1 \mu\text{m}$ . In the second scenario, we examine photodetectors with original lengths ranging from  $1 \mu\text{m}$  to  $4 \mu\text{m}$ .

Our FCNN architecture utilizes blurry electric field measurements as input and outputs the true field profile. It comprises four hidden layers with 800 nodes each, employing Rectified Linear Unit (ReLU) activation functions [7]. We use a learning rate of  $10^{-3}$  and select Adamax as the optimizer [8]. The loss function is defined using mean squared error, and the training process consists of 200 epochs.

Figure 2 displays two sample prediction results of the linear regression and FCNN implementations. Both methods successfully predict the location of the intrinsic layer and the maximum electric field strength ( $|\mathbf{E}|$ ), providing an approximate representation of how  $|\mathbf{E}|$  changes inside the intrinsic region. If we define the relative error as the absolute value of the difference between the true ( $E_{\text{true}}$ ) and predicted ( $E_{\text{pred}}$ ) values divided by the  $E_{\text{true}} + \xi$ , where  $\xi$  is a small positive number to avoid a division by zero error, then the average relative error of both approaches is close to  $0.03 \pm 0.01\%$  and the maximum relative error is  $2.5 \pm 0.3\%$ . However, the linear

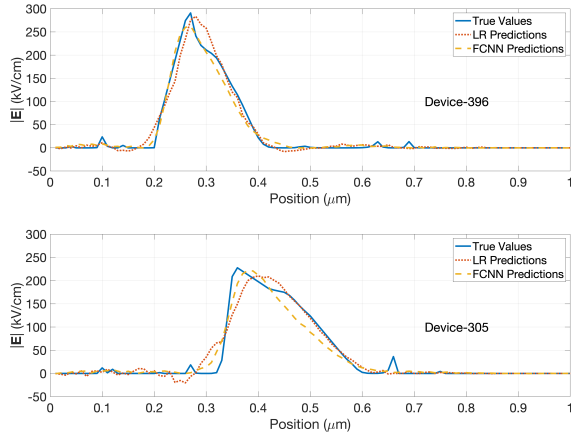


Fig. 2. Comparison of electric field profiles: actual (blue solid curves) vs. predicted using the linear regression model (red dotted curves) and a neural network (orange dashed curves) for two randomly selected photodetectors with a fixed-length of  $1 \mu\text{m}$ .

regression model makes some negative predictions, whereas the FCNN model accurately predicts only positive values. Figure 3 compares the true vs. predicted values corresponding to the (a) left and (b) right boundaries of the photodetector's intrinsic region.

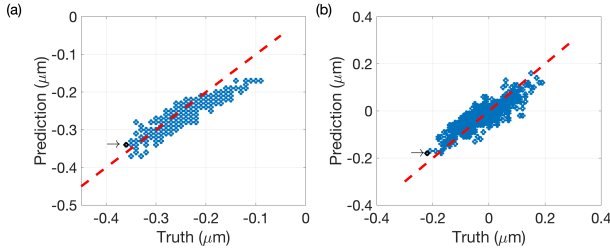


Fig. 3. Each blue circle represents the true vs. predicted value, corresponding to the (a) left and (b) right boundaries of the photodetector's intrinsic region, for one of the 467 unique photodetector designs used for testing. The red dashed line is the  $x = y$  line.

In the second scenario, we examine the photodetectors with their original lengths ranging from  $1 \mu\text{m}$  and  $4 \mu\text{m}$ , i.e.,  $1 \mu\text{m} \leq w_d \leq 4 \mu\text{m}$ . Employing the same machine learning models, we observe that when utilizing 80% of the data for training, we once again achieve highly accurate predictions.

For the results shown in Figures 2, 80% of the data was used for training, with the remaining 20% for testing. To explore the effect of training data size ( $N_{\text{training}}$ ) on accuracy, additional predictions were conducted with  $N_{\text{training}}$  ranging from 10 to 1600. Figures 4(a) and (b) demonstrate how normalized mean squared error changes with  $N_{\text{training}}$  for the first and second scenarios, respectively. The FCNN's accuracy remains nearly constant for  $N_{\text{training}} \geq 100$ , whereas the linear regression model exhibits significant errors for smaller  $N_{\text{training}}$ . This suggests that linear regression becomes less reliable when the training and testing datasets have low correlations or when the

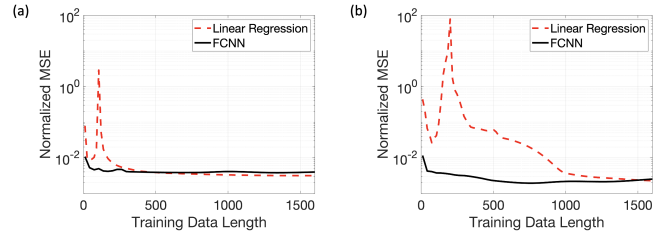


Fig. 4. Normalized mean squared error as a function of training data set size for linear regression (red dashed curve) and an FCNN (black solid curve) for a data set with devices of (a) constant length and (b) varying length.

training data significantly differs from testing data. The neural network's multiple layers and numerous neurons enable it to learn underlying patterns effectively, even with limited training data.

### III. CONCLUSION

We explore the use of machine learning techniques for enhancing LNFP measurement resolution, particularly when the probe size exceeds that of the device under investigation, yields several key findings: (i) neural networks achieve  $\lambda/10$  spatial resolution even with probes of only a few wavelengths, maintaining a maximum relative error of less than 3%, (ii) Fully connected neural networks outperform linear regression models with small training datasets, and (iii) for extensive training datasets, constructing and training neural networks may be unnecessary; linear regression proves sufficient and efficient. These results suggest the applicability of similar machine learning approaches to improve resolution in various measurement setups.

### REFERENCES

- [1] S. K. Dutta, C. P. Vlahacos, D. E. Steinhauer, Ashfaq S. Thanawalla, B. J. Feenstra, F. C. Wellstood, S. M. Anlage, and H. S. Newman, "Imaging microwave electric fields using a near-field scanning microwave microscope," *Appl. Phys. Lett.*, vol. 74, no. 1, pp. 156–158, 1999.
- [2] R. Kantor and I. V. Shvets, "Measurement of electric-field intensities using scanning near-field microwave microscopy," *IEEE Trans. Microw. Theory Tech.*, vol. 51, no. 11, pp. 2228–2234, Nov. 2003.
- [3] D.W. Pohl, L. Novotny, B. Hecht, and, H. Heinzelmann, "Radiation coupling and image formation in scanning near-field optical microscopy," *Thin Solid Films*, vol. 273, no. 1–2, pp. 161–167, 1996.
- [4] R. Dian, S. Li, A. Guo and L. Fang, "Deep Hyperspectral Image Sharpening," *IEEE Transactions on Neural Networks and Learning Systems*, vol. 29, no. 11, pp. 5345–5355, Nov. 2018.
- [5] E. Simsek, I. Md Anjum, T. F. Carruthers, C. R. Menyuk, J. C. Campbell, D. A. Tulchinsky, K. J. Williams, "Fast Evaluation of RF Power Spectrum of Photodetectors with Windowing Functions," *IEEE Electron Dev.*, vol. 70, no. 7, pp. 3643–3648, 2023.
- [6] E. K. Cho and E. Simsek, "Enhancing the Resolution of Local Near-Field Probing Measurements with Machine Learning," *IEEE Trans. Microw. Theory Tech.*, Sept. 2023. DOI: 10.1109/TMTT.2023.3312036
- [7] V. Nair and G. E. Hinton, "Rectified linear units improve restricted Boltzmann machines," *ICML'10: Proceedings of the 27th International Conference on International Conference on Machine Learning*, pp. 807–814, June 2010.
- [8] D. P. Kingma and J. Ba, "Adam: A Method for Stochastic Optimization," *arXiv:1412.6980*. Date of access: 11/06/2022.
- [9] Resolution Data Set. Available: <https://github.com/simsekergun/Resolution>